



Article

Photocatalytic Advanced Oxidation Processes for Neutralizing Free Cyanide in Gold Processing Effluents in Arequipa, Southern Peru

David C. Vuono ¹, Johan Vanneste ¹, Linda A. Figueroa ¹ , Vincent Hammer ¹, Fredy N. Aguilar-Huaylla ², Aaron Malone ³, Nicole M. Smith ³, Pablo A. Garcia-Chevesich ^{1,4}, Héctor G. Bolaños-Sosa ⁵, Francisco D. Alejo-Zapata ⁶ , Henry G. Polanco-Cornejo ^{5,*} and Christopher Bellona ^{1,*}

¹ Department of Civil and Environmental Engineering, Colorado School of Mines, Golden, CO 80401, USA; dvuono@mines.edu (D.C.V.); vanneste@mines.edu (J.V.); lfigueroa@mines.edu (L.A.F.); vhammer@mymail.mines.edu (V.H.); pchevesich@mines.edu (P.A.G.-C.)

² School of Metallurgical Engineering, National University of San Agustín, Arequipa 04000, Peru; fredy_aguilarrh@hotmail.com

³ Department of Mining Engineering, Colorado School of Mines, Golden, CO 80401, USA; amalone@mines.edu (A.M.); nmsmith@mines.edu (N.M.S.)

⁴ International Hydrological Program—IHP, UNESCO, Montevideo 11200, Uruguay

⁵ School of Chemistry, National University of San Agustín, Arequipa 04000, Peru; hbolanos@unsa.edu.pe

⁶ School of Process Engineering, National University of San Agustín, Arequipa 04000, Peru; falejo@unsa.edu.pe

* Correspondence: hpolancoc@unsa.edu.pe (H.G.P.-C.); cbellona@mines.edu (C.B.); Tel.: +51-942-503-982 (H.G.P.-C.); +1-303-273-3061 (C.B.)



Citation: Vuono, D.C.; Vanneste, J.; Figueroa, L.A.; Hammer, V.; Aguilar-Huaylla, F.N.; Malone, A.; Smith, N.M.; Garcia-Chevesich, P.A.; Bolaños-Sosa, H.G.; Alejo-Zapata, F.D.; et al. Photocatalytic Advanced Oxidation Processes for Neutralizing Free Cyanide in Gold Processing Effluents in Arequipa, Southern Peru. *Sustainability* **2021**, *13*, 9873. <https://doi.org/10.3390/su13179873>

Academic Editor: Glen Corder

Received: 20 July 2021

Accepted: 27 August 2021

Published: 2 September 2021

Publisher's Note: MDPI stays neutral with regard to jurisdictional claims in published maps and institutional affiliations.

Abstract: Cyanide (CN^-) from gold processing effluents must be removed to protect human health and the environment. Reducing the use of chemical reagents is desirable for small centralized and decentralized facilities. In this work, we aimed to optimize the use of ultraviolet (UV) radiation coupled with hydrogen peroxide (H_2O_2) to enhance the rate and extent of CN^- removal in synthetic and actual gold processing effluents, from one centralized and one decentralized facility in southern Peru. Bench-scale studies conducted using H_2O_2 and ambient UV showed no significant effects on CN^- destruction; however, experiments with higher UV intensity and H_2O_2 accelerated free CN^- degradation. When a 1:1 stoichiometric ratio of CN^- : H_2O_2 was tested, the highly concentrated effluent (1 g CN^- /L) had a slower pseudo first-order rate constant ($k = 0.0066 \text{ min}^{-1}$) and took ~5 h longer to reach 99% destruction, compared with the low concentration effluent (100 mg CN^- /L; $k = 0.0306 \text{ min}^{-1}$). Lastly, a TiO_2 photocatalyst with low stoichiometric CN^- : H_2O_2 ratios (1:0.1 and 1:0.2), in a compound parabolic solar concentrator, was tested to investigate the degradation of a high concentration effluent (1.28 g CN^- /L). These results show a significant improvement to degradation rate within a 20 min period, advancing treatment options for mineral processing facilities.

Keywords: cyanide; cyanidation; gold mining; advanced oxidation process; photocatalyst; hydrogen peroxide; titanium dioxide; Arequipa; Peru; mining water treatment

1. Introduction

In 2019, Peru was the largest producer of gold in Latin America and the 8th largest producer of gold in the world [1]. The Arequipa region in south-western Peru, accounts for 14.6% of gold production along with the highest share of mining employment. This region also produces the third highest output of gold from artisanal and small-scale operations in the country [1]. Despite the economic importance of gold production, the environmental impacts of extraction operations on surface and groundwater quality and human health have become a primary concern in Peru [2–6]. Growth in gold extraction has brought increased social conflicts, often centering on water supply and, most commonly, water contamination [7–9]. This is particularly important in Arequipa, one of Peru's most arid



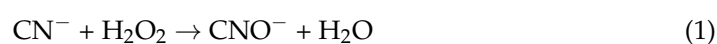
Copyright: © 2021 by the authors. Licensee MDPI, Basel, Switzerland. This article is an open access article distributed under the terms and conditions of the Creative Commons Attribution (CC BY) license (<https://creativecommons.org/licenses/by/4.0/>).

regions, barely receiving 75 mm of mean annual rainfall concentrated during summer months [10]. Conflicts over the effects of gold extraction on water pollution has in some instances pitted mining against agriculture, another leading economic sector and the main water consumer [9]. The combined strains of Arequipa's arid climate and water demands pose challenges to mining sustainability due to ineffective or lacking water treatment, water reuse, resource recovery, and conflict resolution.

Recent extreme degradation of surface water quality in the Arequipa region, such as the cases of Tambo, Chili, Ocoña, and Coralque rivers, particularly with regard to heavy metals contamination and cyanide spills [11], have pointed to potential impacts from mining-related activities [12]. Even with efforts from the Peruvian government to develop water quality regulations for human consumption and environmental quality standards for water [13,14], administrative mechanisms to enforce poor corporate environmental practices are needed [15]. This has led to proactive measures aiming to develop sustainable mining practices at established mines and mineral processing facilities, such as the Cerro Verde copper mine, where access to water for mining expansion was granted in exchange for treating the municipal sewage from the city of Arequipa [16].

Conventional mineral-processing facilities in the Arequipa region primarily use the cyanidation process for dissolution of gold-containing ores [1]. However, after cyanide-gold complexes are removed (e.g., adsorption with activated carbon), the residual cyanide-rich effluents are commonly poorly treated prior to reuse or discharge. The mineral processing operations in this arid region typically send their cyanide containing effluents to large evaporation ponds to undergo sedimentation and passive exposure to ultraviolet (UV) irradiation before being reused onsite for additional batch processing. However, significant progress can be made to optimize chemically based treatment processes for centralized and decentralized operation facilities, which often differ in their water quality, types of available utilities, and onsite resources. Treatment processes such as advanced oxidation may be used process reuse, discharge, or nutrient recovery, depending on local needs and these processes can be further optimized to reduce chemical consumption.

Cyanide can be degraded using a variety of advanced oxidation processes (AOP). Hydrogen peroxide is routinely used for converting free and weak acid dissociable metal-cyanide complexes into the much less toxic cyanate [17], according to the following reactions:



where Reaction (1) is optimal under alkaline conditions and the end-product, cyanate, can hydrolyze into ammonium (Reaction (2)), a process that can be faster under acidic conditions [17–19]. When peroxide is combined with UV, two hydroxyl (OH) radicals are formed by homolytic cleavage of the central HO–OH bond [20]. While two ·OH radicals are formed, only one is able to participate in the AOP because the second one is surrounded by water molecules in a solvent cage [21]. Despite the one-to-one stoichiometric effectiveness of UV/H₂O₂, this process has been shown to be effective for treating cyanide-containing effluents [22,23] and is preferred over other AOPs, such as ozone, because peroxide is relatively inexpensive, water soluble, and simple to store and handle [18]. UV irradiation in combination with hydrogen peroxide (H₂O₂) is also a particularly attractive treatment option [24], as the Arequipa region receives high solar radiation ranging between 850 to 950 W/m² and a UV intensity of ~0.2 mW/cm², which may be used in place of UV lamps [25]. Titanium dioxide (TiO₂) photocatalysts have also been used to accelerate degradation in cyanide containing effluents [26,27], although with varying degrees of success. The major end-products of cyanide destruction using TiO₂ are cyanate, nitrite, and nitrate [26,27], which feed the nitrogen cycle [28]. Mechanistically, when TiO₂ is excited by UV light, an electron hole is created on CN[−] and on water molecules, which generates ·OH radicals for further oxidative degradation [29,30]. However, due to the low quantum

yield for $\cdot\text{OH}$ radical generation, UV/ TiO_2 alone is typically not considered an efficient AOP [31].

The aim of this investigation was to evaluate the effectiveness of alternate UV sources (ambient UV versus a UV lamp), optimize the dosing requirements of peroxide at different cyanide concentrations, and evaluate the effectiveness of a TiO_2 photocatalyst, to provide treatment guidelines for the various types of mineral processing facilities (centralized versus decentralized) in the Arequipa region. To accomplish this, we obtained water quality data from two mineral processing facilities with different site characteristics in the Arequipa region. The first processing plant, called La Quinta, operating near the town of Vitor was chosen for its remote location and geographic distance from centralized utilities, where water and chemicals are transported to the site. The second plant, called Cepromet Minera Porvenir S.A.C. (hereafter referred to as Cepromet), is in a suburb outside of Arequipa city and was chosen as a counterpart to La Quinta for its proximity to centralized utilities. La Quinta also processes ore from a single site, whereas Cepromet processes ore from a variety of locations, depending on demands. Both sites reuse their processed water but without further treatment or water purification, which may affect process efficiency and may contaminate local water resources if spilled. Three experiments were conducted with synthetic cyanide-containing wastewater of similar concentrations to those found at the two previously mentioned processing facilities: (1) UV only; (2) peroxide with ambient UV ($0.2 \text{ mW}/\text{cm}^2$); and (3) peroxide with $4.6 \text{ mW}/\text{cm}^2$ UV intensity at total cyanide concentrations of $\sim 1000 \text{ mg}/\text{L}$ and $\sim 100 \text{ mg}/\text{L}$, all to elucidate the effects of cyanide concentration on destruction rate. Additionally, a fourth experiment was performed treating real cyanide-containing wastewater from Cepromet using a low ratio of cyanide:peroxide (1:0.1 and 1:0.2) in combination with TiO_2 in a compound parabolic concentrator (CPC) with an approximate intensity of $0.4 \text{ mW}/\text{cm}^2$.

2. Materials and Methods

2.1. Site and Processing Characteristics

At the La Quinta mineral processing facility, ore transported from a local mine is ground to about $76 \mu\text{m}$ using a ball mill. Fresh water for the process is trucked in from the Vitor River and stored in an open lined pond prior to use. Approximately $4 \text{ kg CN}/\text{Mg}$ of ore is used for each batch, which occurs in two 30 m^3 reaction tanks in series. After cyanide reacts with ground ore for approximately 36 h, the water is pumped through granular activated carbon (GAC) supported on a mesh screen with 20 kg of GAC used per m^3 of metal/cyanide-containing process water. This facility processes intrusive rocks of monzotonalite composition, belonging to the Punta Coles super unit of the Cordillera de La Costa. La Quinta has a daily treatment capacity of 25–30 Mg of gold ore, with the ore containing $\sim 5\text{--}10 \text{ g}$ of gold/Mg of ore. It is estimated that $\sim 90\%$ is recovered using this process (personal communication). After the gold–cyanide complexes have been adsorbed onto GAC, the waste effluent is pumped to a lined retention pond where sedimentation occurs. Clarified effluent is then pumped and stored in two $\sim 15 \text{ m}^3$ storage tanks prior to reuse.

At the Cepromet facilities, on the other hand, four tanks in series (total volume of 22 m^3) are used in the cyanidation process and allowed to react for 3 days. Similar to La Quinta, $4 \text{ kg CN}^-/\text{Mg}$ of ore are also used for each batch. After the reaction is complete, 20 kg of GAC are used for every m^3 of concentrate to retain the cyanide–gold complexes. The cyanide–gold slurry is then passed through a trommel used to separate GAC from the slurry. The waste effluent is then transferred to a lined retention pond that is covered by a large solar shade, where it sits for sedimentation and is thereafter transferred to a concrete storage basin to be reused for future batches without any additional treatment.

2.2. Sampling

Water used in the cyanidation process was collected from the waste tanks at each facility using a sampling tube (1/2" outside diameter), connected to a cordless drill-powered pump (Wayne Company, Harrison, OH, USA) and filtered through a 0.45 μm inline filter. Fifty ml of cyanide-containing water were collected for each sample analysis. For total cyanide, samples were field-adjusted to pH 12 using standard protocols [17]. A hydrogen cyanide gas detector was used to warn against exposure (BW Technologies).

2.3. Sample Analysis

Total cyanide was measured using Hach Test N' Tube (TNT) 862 pyridine barbituric acid method (Hach, Loveland, CO, USA). Dissolved organic carbon (DOC) was measured using a total organic carbon (TOC) TOC-L analyzer (Shimadzu, Columbia, MD, USA). Total nitrogen (TN) was evaluated simultaneously with TNM to run the ASTM D 8083 method by high-temperature catalytic combustion and chemiluminescent detection. Ammonia was measured using Hach TNTplus 831 by salicylate method (Hach, Loveland, CO, USA). For cyanide destruction end-product analysis involving the experiment with low/high cyanide concentrations, the end-point sample pH was lowered to 2.5 with 1% (*v/v*) sulfuric acid. Inorganic anions were measured using ion chromatography (Dionex 1500, Sunnyvale, CA, USA), with IonPac AS14 and guard columns. Alkalinity was measured using the titration 8203 method (model 16900, Hach, Loveland, CO, USA). Elemental analysis was carried out by inductively coupled plasma-optical emission spectroscopy (ICP-OES) (Avio-500, Perkin-Elmer, Fremont, CA, USA).

2.4. Experimental Design

2.4.1. Batch Experiments at Ambient UV Intensity

Oxidant experiments (hydrogen peroxide 30% *w/w* in H_2O ; Sigma-Aldrich, St. Louis, MO, USA) with simulated natural UV radiation were accomplished using 100 mL volume batches in 1 L fused-quartz Erlenmeyer flasks (Technical Glass Products Inc, Painesville, OH, USA) on a NEST array (Lumenautix, LLC, Reno, NV, USA), following the procedure by Read et al. [32]. Briefly, this array is comprised of multiple discrete solid-state emitters operating in two modes, VIS and UV, connected to a control unit. The output is regulated, and temperature compensated for constant DC current, which allows for precise control and stability of light output. Visible light emitting diodes (LEDs) are blue ($n = 3$), red ($n = 3$), and white ($n = 6$), while the UV devices emit at 285 nm ($n = 3$, UVB range). For this investigation, only the UV emitters with an irradiance of 0.2 mW/cm^2 were used.

2.4.2. Batch Experiments with Recirculation and Medium-Intensity UV Lamp

To test the effectiveness of an intensity UV source higher than the intensity of natural UV and the impact of hydrogen peroxide (30% *w/w* in H_2O ; Sigma-Aldrich, St. Louis, MO, USA), a 3.3 L automated UV-based cyanide-destruction batch reactor was constructed (Figure 1). A residential UV lamp was chosen because it is an off-the-shelf item that can be easily obtained in Peru by local vendors, in addition to the fact that it is powerful enough to activate hydroxyl radicals [21]. The UV lamp emits at 254 nm with an energy density of 40 mJ/cm^2 measured by the manufacturer at a flow rate of 8.3 LPM (Lumenor, Guelph, ON, Canada) and a working volume of 1.2 L. The power density, which is independent of the flowrate, can be calculated based on the energy density measured at a given flowrate. For example, at a flowrate of 8.3 LPM and a lamp's working volume of 1.2 L, the residence time in the device is 7.9 s. Dividing the reported energy density by the residence time yields a 4.6 mW/cm^2 energy density.

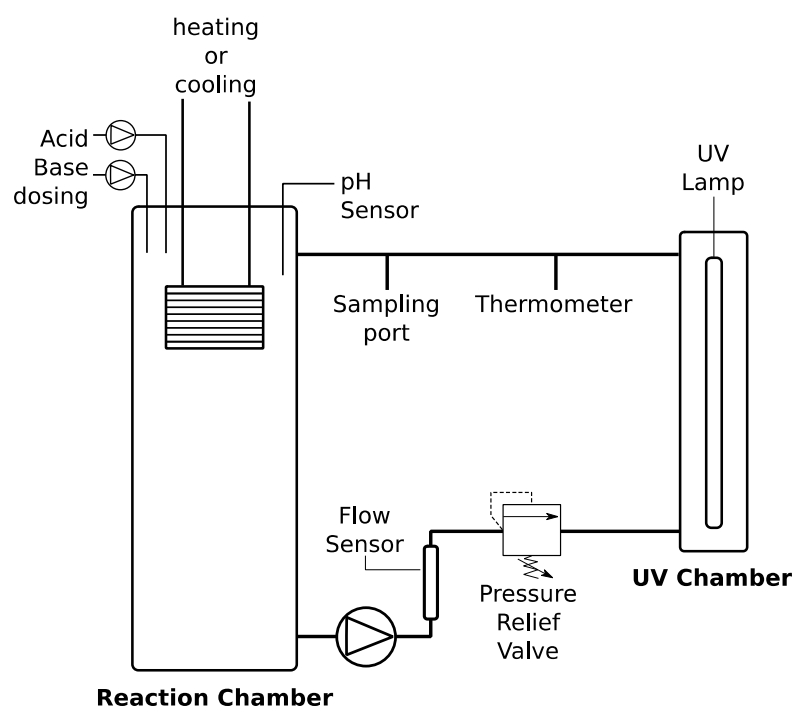


Figure 1. Process flow diagram of the automated pilot system (not to scale).

The system is also equipped with sensor ports for online pH monitoring and is temperature controlled (IsoTemp 3006, Fischer Scientific, Waltham, MA, USA) by a virtual interface (VI) programmed in LabView (hosted on the user's laptop). The system is gas tight and was pressure tested prior to experimentation and is also equipped with pH control by dosing with 0.1 M sulfuric acid and 0.1 M sodium hydroxide. Oxidant dosing is also configured; however, manual dosing was used in oxidant-to-cyanide ratio experiments.

2.4.3. Batch Experiment with Compound Parabolic Concentrator

A compound parabolic concentrator (CPC) was used to direct solar radiation for field studies conducted with real cyanide effluent at the Cepromet mineral-processing facility. The CPC consists of a metal base that supports an array of three non-UV absorbing acrylic tubes (85 cm long and 4.36 cm inside diameter) that are superimposed on a metal support structure with an aluminum reflective surface. A 30° inclination plane was used according to the latitude of Arequipa during summer season (December–February). Available UV-B power density in January for southern Peru is around 0.2 mW/cm² [33]. Based on the dimensions of the CPC (10 cm diameter), a concentration factor of 2 can be achieved, yielding an effective power density of 0.4 W/m². For each CPC, a 1 L volume was used during experimental testing. With this configuration, the effect of concentrated ambient UV was tested with peroxide (14.31% w/w in H₂O; Sigma-Aldrich, St. Louis, MO, USA) at two peroxide concentrations 1 mL and 2 mL peroxide/L of cyanide solution (1280 mg free CN[−]/L; ratios 1:0.1 and 1:0.2, respectively) and a titanium dioxide photocatalyst at two catalyst concentrations: 50 mg/L and 500 mg/L TiO₂. The photocatalyst used in this study was a rutile titanium dioxide semiconductor with a 0.23 μm average particle size and was recovered after each experiment. Photocatalyst concentrations of 50 mg/L and 500 mg/L were used to prevent optical shielding that is known to occur at higher concentrations [27]. Real cyanidation effluent from the Cepromet plant was used. The control for the experiment consisted of cyanidation effluent in the absence of TiO₂ to establish baseline conditions. An additional experiment was conducted to provide a central point among the three independent variables: irradiation time (synonymous with runtime), peroxide concentration, and TiO₂ concentration (mg TiO₂/L CN[−] containing waste). These values were 130 min irradiation, 1.5 mL peroxide/L of cyanide solution (ratio 1:0.14), and

275 mg/L TiO_2 . This served to create a 2^3 factorial design with 8 experimental tests and 3 replicates at the central point.

2.4.4. Data Analysis

Destruction rates were calculated as $r = ((C_0 - C_1)/(t_1 - t_0)) \times \text{volume}$, where C_0 and C_1 are the corresponding concentrations for each timepoint, t_0 is the starting timepoint when hydrogen peroxide was dosed, and t_1 is the subsequent point. Rate constants were estimated by adjusting the rate constant such that the sum of the squared error between modeled and measured data was maximized with a non-linear approach using Equation (3), where C_0 is the concentration at time t_0 , k is the rate constant, and t_n is the time at each sampling timepoint.

$$C_0 \times e^{-kt_n} \quad (3)$$

3. Results

3.1. Field Data

Effluent from each mineral processing facility was successfully collected from waste storage tanks to characterize effluent water quality for treatment purposes (Figure 2). Mean pH values for La Quinta and Cepromet were 10.5 and 9.65, respectively as well as mean total cyanide concentrations of 92 mg/L CN^- and 1055 mg/L CN^- , respectively. Other notable analyte differences between the two sites were lower concentrations of TN, DOC, copper, boron, fluoride, arsenic, selenium, magnesium, molybdenum, and lead at La Quinta. These results enabled us to design synthetic cyanide solutions at two concentrations for laboratory experimentation. However, a number of contaminants measured in cyanide-containing effluents exceeded the Peruvian environmental quality standards, including arsenic, boron, iron, copper, and lead (at Cepromet). This indicates that destruction of cyanide from these waters alone is insufficient for (e.g.,) surface water discharge and thus further treatment is needed to elevate water quality for reuse or discharge.

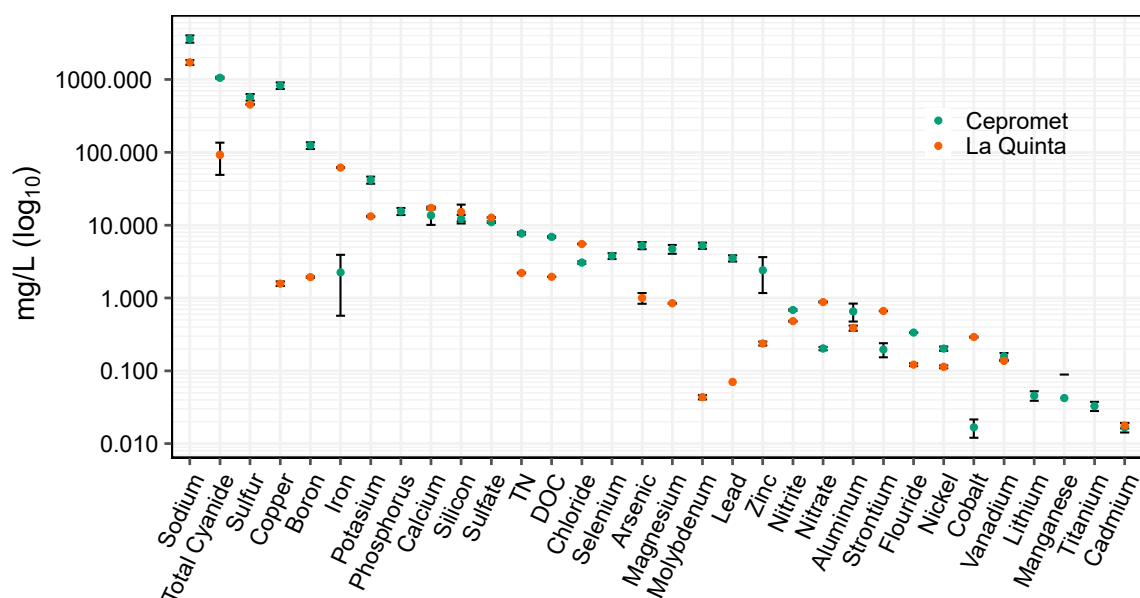


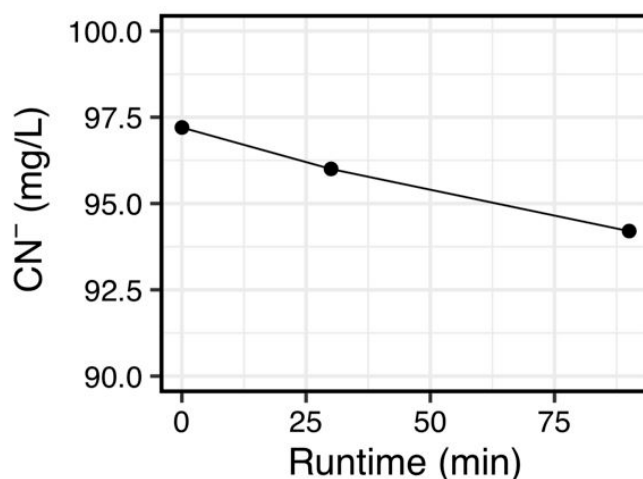
Figure 2. Water quality characterization of the two gold-processing sites in the Arequipa region. La Quinta represents a remote mine site that treats ore from a single source, whereas Cepromet is a centralized facility that processes ore from a variety of sources. Analytes are ordered from highest concentration to lowest on a \log_{10} scale. Error bars represent standard deviation.

3.2. Effects of UV and Peroxide as a Function of Free Cyanide Concentration and Peroxide Ratio Using Synthetic Solution

Post ore processing effluent is sent to holding ponds for passive treatment (i.e., sedimentation, ambient UV oxidation) prior to discharge or reuse for the two facilities studied, as previously mentioned. To evaluate the effectiveness of utilizing UV radiation in natural sunlight as a passive method to accelerate cyanide destruction, a NEST array, to simulate low intensity natural UV-B (285 nm) radiation at 0.2 mW/cm^2 , was employed in batch. Initial cyanide of $\sim 97 \text{ mg/L}$ with 1:0.1 ratio of $\text{CN}^-:\text{H}_2\text{O}_2$ demonstrated only 1.9% destruction over a 90-min reaction time (Figure 3a). These results indicate that ambient UV radiation irradiance is not feasible for rapid cyanide destruction, even in the presence of added peroxide.

A batch system with recirculation and a higher UV irradiance (4.6 mW/cm^2) was subsequently employed at low initial cyanide concentration ($\sim 90 \text{ mg/L CN}$) with UV alone (Figure 3b), and peroxide addition with and without UV (Figure 3c). The effectiveness of UV irradiation alone on cyanide destruction was evaluated at ambient temperature (25°C), as shown in Figure 3b, and no change in initial cyanide concentration was observed after an 8-h period, indicating that a 10-fold increase in UV irradiation (relative to ambient UV irradiation) was still insufficient to destroy cyanide in solution.

The effects of peroxide without and with UV on cyanide destruction was tested for an initial concentration of $\sim 100 \text{ mg/L CN}^-$. The experimental results are characterized by “Phase”, based on reactant condition and time (Figure 3c). The experiment tested the effects of peroxide alone and peroxide with UV on cyanide destruction. Hydrogen peroxide was dosed at a 1:0.1 stoichiometric ratio (cyanide to peroxide), at the beginning of the experiment, with a circulation rate of 1 L/min to provide mixing. Percent decreases in cyanide concentration are expressed as a percent of initial values. In Phase I, the reactor mixed for 140 min with cyanide and peroxide and with the UV lamp turned off, observing a 4% decrease in cyanide concentration. The high-intensity UV lamp was turned on at 140 min for 120 min (Phase II). The combination of peroxide and UV resulted in an initial 18.3% decrease in cyanide concentration.



(a)

Figure 3. Cont.

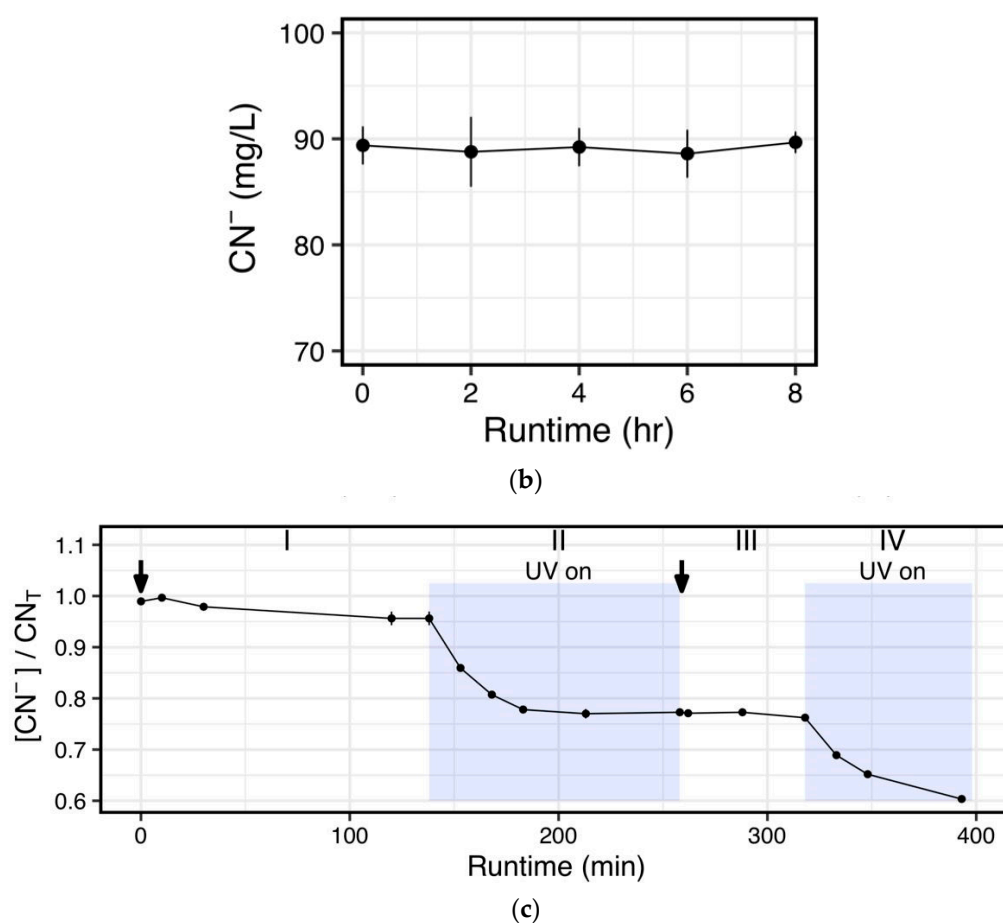


Figure 3. Initial batch experimentation to test: (a) cyanide destruction with 1:0.1 dose of cyanide: H_2O_2 and ambient UV from the NEST system. This system has the UV strength intensity of natural sunlight ($\sim 0.2 \text{ mW}/\text{cm}^2$ at a wavelength of 285 nm to be in the UVB range). (b) Effects of a UV lamp on the destruction of cyanide over time. (c) Effects of peroxide on cyanide destruction (100 mg/L starting concentration) over time, successively dosed at 1:0.1 stoichiometric ratios in combination with a UV lamp. In (c), light blue boxes indicate when the UV lamp was turned on (Phases II and IV).

Hydrogen peroxide was added again at a 1:0.1 stoichiometric ratio (based on remaining cyanide concentration) and allowed to mix for 60 min with the UV lamp turned off (Phase III), observing a 1% decrease in cyanide concentration during this Phase (peroxide alone). The last 75 min of the experiment demonstrated that peroxide and UV together provided an additional 15.9% decrease in cyanide concentrations (Phase IV). In total 39.3% destruction of cyanide was observed, of which 34.2% was attributed to the combination of UV light and peroxide (Phases II and IV). Together, the results above demonstrate the importance of combining UV with peroxide to accelerate degradation of free cyanide.

The combination of UV (at $4.6 \text{ mW}/\text{cm}^2$) and peroxide was shown to promote cyanide destruction (Figure 3c). Thus, experiments to elucidate the rate of cyanide with UV/ H_2O_2 were conducted with high ($\sim 1000 \text{ mg}/\text{L}$) and low ($\sim 100 \text{ mg}/\text{L}$) initial cyanide concentrations with stoichiometric additions of peroxide (Equation (1)). Removal of cyanide at a 1:1 dose of peroxide to cyanide showed 99.9% and 98.9% removal for low and high initial cyanide concentrations, respectively (Figure 4a). The pseudo first-order rate constant was higher at low cyanide concentration relative to the higher initial concentration: $k = 0.0306 \text{ min}^{-1}$ and $k = 0.0066 \text{ min}^{-1}$, respectively. The initial rate of cyanide removal at high concentration was slightly superior to the low cyanide concentration: $3\text{--}6 \text{ mg CN}^- \text{ L}^{-1} \text{ min}^{-1}$ versus $1.5\text{--}3 \text{ mg CN}^- \text{ L}^{-1} \text{ min}^{-1}$, respectively (Figure 4b). In summary, effective removal of cyanide required medium UV intensity in conjunction with

stoichiometric peroxide. Batch incubation times required for cyanide destruction were 2 to 8 h for low and high initial cyanide concentrations, respectively.

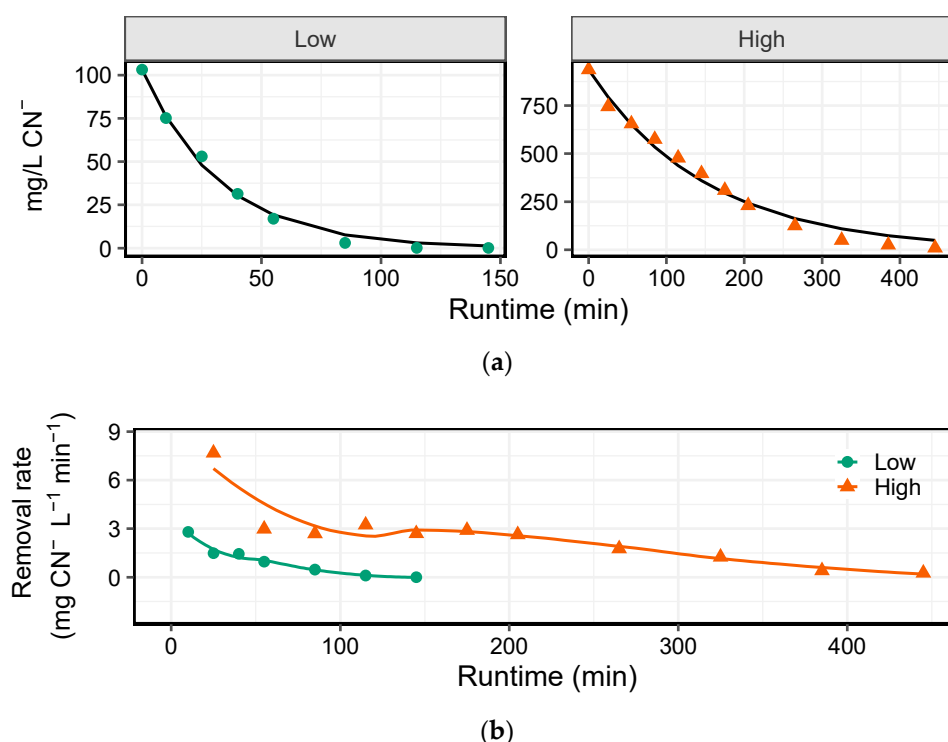


Figure 4. (a) Cyanide destruction at two initial concentrations (Low = 100 mg/L CN⁻ & High = 1 g/L CN⁻) with 1:1 stoichiometric ratio of initial cyanide to hydrogen peroxide. Black curve indicates the model fit and dots indicate the mean of measured time-points. (b) Cyanide removal rate over time for low and high cyanide concentrations. Smoothed curves indicate a locally weighted regression and ribbons represent standard errors.

3.3. Effect of Titanium Dioxide with Low CN⁻:H₂O₂ Ratios on the Destruction of High Initial Cyanide Concentrations in CPC Using Real Cyanide Solution

The effect of concentrated ambient light in a CPC with peroxide in combination with a titanium dioxide photocatalyst was evaluated at two catalyst concentrations, 50 mg/L and 500 mg/L TiO₂ and two peroxide doses, 1:0.1 and 1:0.2 stoichiometric ratio of CN⁻:H₂O₂ (Figure 5). Total initial cyanide concentration was 1292 mg/L and free cyanide concentration was 1280 mg/L. The TiO₂ catalyst and above stoichiometric cyanide:peroxide ratio was expected to increase the rate and extent of cyanide degradation, greater than what was observed for ambient UV with peroxide and high UV irradiance with peroxide. No significant destruction of cyanide was observed in the controls (~3.1%) over four hours. The maximum extent of cyanide destruction with TiO₂ and peroxide occurred by the time the first sample was taken at 20 min (Figure 5). A tenth of the stoichiometric addition (1:0.1) of peroxide resulted in free cyanide destructions of 57% ± 3.4% and 57.7% ± 2.5%, at 50 mg/L and 500 mg/L TiO₂, respectively. The effect of a twentieth stoichiometric peroxide addition (1:0.2) significantly improved degradation, but like the 1:0.1 CN⁻:H₂O₂ dose, higher TiO₂ concentrations appeared to only provide a minor improvement to degradation at both peroxide doses (see Figure 5). At a 1:0.2 peroxide dose, free cyanide destruction of 82.1% ± 5.2% and 89.9% ± 1.9% at 50 mg/L and 500 mg/L TiO₂, respectively, was observed. Additional experiments were performed to test the effects of copper-catalyzed destruction in the presence of peroxide (see SI). These experiments were performed to ascertain if copper in solution, in combination with added peroxide and UV, had any effect on cyanide destruction, showing no significant effect of copper dioxide on cyanide destruction (Figure S1 in the Supplementary Materials). In summary, experimental analysis

of peroxide dose versus TiO_2 concentration revealed maximum removal in under 20 min with a 1:0.2 peroxide dose that was marginally improved when 500 mg/L TiO_2 was used over 50 mg/L TiO_2 . These results indicate a significant improvement to the chemical requirements needed to achieve higher cyanide destruction rates with a CPC.

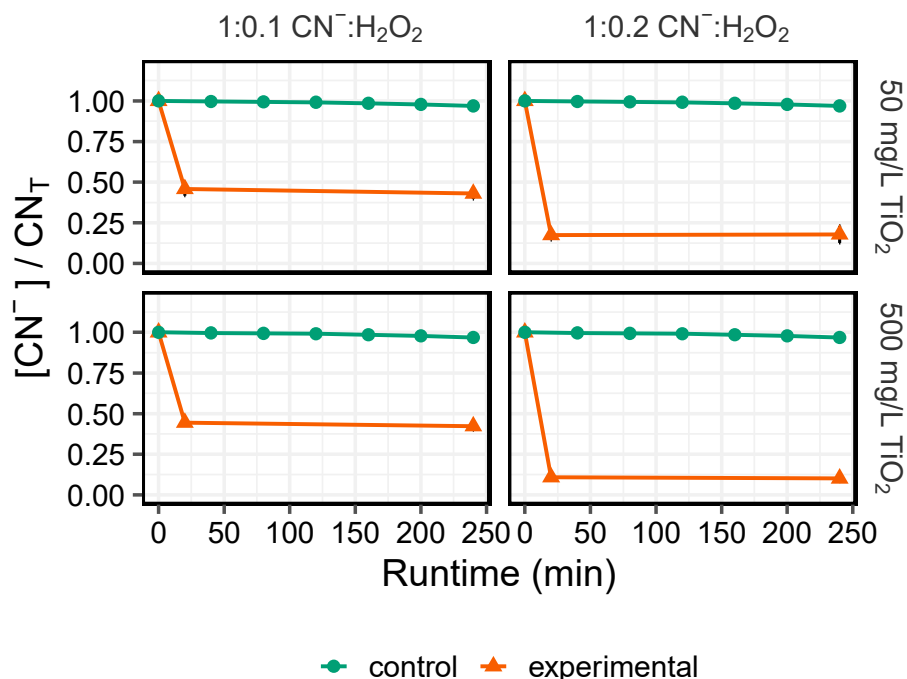


Figure 5. Free cyanide destruction as a function of peroxide dose (columns) and titanium dioxide concentration (rows) over time. The control group tests the effects on cyanide destruction with UV without TiO_2 and peroxide.

In the TiO_2 experiments, we observed that (1) degradation occurred rapidly (within 20 min); (2) peroxide dose appeared to significantly improve removal of cyanide; and (3) higher TiO_2 concentration provided a minor improvement for degradation. Data from the TiO_2 experiments were statistically evaluated using multiple linear regression analyses (Figure 6). This design enabled the assessment of the statistical significance of the primary variables but also evaluated the significance of the interaction terms (i.e., the combination of variables on % CN^- removal). Results show that when the linear model included only the main effects (i.e., irradiation time, peroxide concentration, and TiO_2 concentration), peroxide dose was highly significant ($p < 0.001$) and TiO_2 concentration was moderately significant ($p = 0.0243$) with the model explaining 91.3% of the variance in the data ($R^2 = 0.913$). These results suggest that the interaction terms might also play a role in free cyanide removal, particularly the interaction between peroxide concentration and TiO_2 concentration. Results show only minor support for an interaction effect of peroxide concentration and TiO_2 concentration on free cyanide removal ($p = 0.08$). This indicates that higher concentrations of TiO_2 are not needed for treating high strength cyanide-containing effluents.

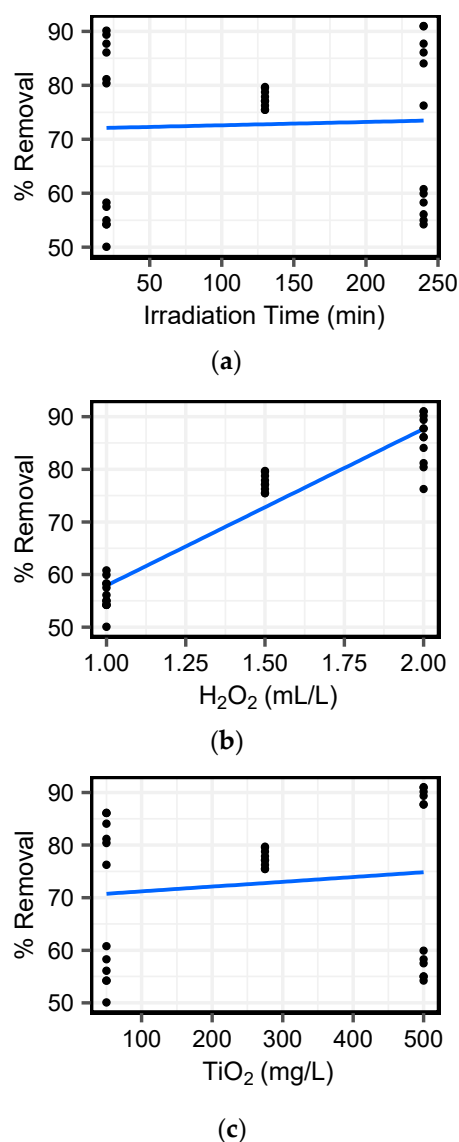


Figure 6. Linear regression for main variables (a) irradiation time, (b) peroxide concentration (3%), and (c) TiO_2 concentration, on free cyanide removal (%).

4. Discussion

The aim of this investigation was to evaluate water treatment options for two geographically disparate mineral processing facilities in the Arequipa region of southern Peru: a remote site that processes ore from a single mine location (La Quinta), and a centralized facility that receives ore from various sources (Cepromet). First, we characterized the water quality of each site to determine viable treatment options (Figure 2). Based on these results, which revealed an order of magnitude difference in cyanide concentrations, three treatment options were tested: (1) a 1:0.1 dose of peroxide in combination with low UV strength of intensity similar to natural sunlight (Figure 3a); (2) a 1:0.1 dose of peroxide and a UV lamp (Figure 3c), and a 1:1 dose of peroxide with a UV lamp (Figure 4); and (3) CPC-concentrated UV with peroxide, in combination with a TiO_2 photocatalyst to accelerate degradation of high strength cyanide containing effluents using minimal peroxide (Figures 5 and 6).

Peru is a mining epicenter with increasing concerns about the sustainability of mining-related activities and their effects on water resources and livelihoods [6]. The environmental impacts pertaining to the lack of water treatment in Peruvian gold mining are additionally challenging because many artisanal and small-scale mining operations use mercury to extract gold from ore [34]. Tailings from mineral processing with mercury are often sold to

processing facilities (e.g., Cepromet) for further gold extraction using cyanide, leading to a treatment challenge, as mineral processing facilities may not only treat ore from different sites, but also often treat ore that has been previously treated with mercury. While mercury concentrations were not measured in this study, there is significant evidence for mercury use in surrounding regions [5,35] and in the Arequipa territory. Thus, the ore may have different mineralogical and chemical compositions, thus affecting post-cyanidation water quality. Furthermore, cyanide processing of mercury-contaminated tailings creates Hg-CN^- complexes that are highly toxic and bioavailable [36]. When Cepromet's water quality was characterized, it was found that it contained an order of magnitude higher cyanide concentration than the remote site (La Quinta), and had significantly higher concentrations of TN, TOC, copper, boron, fluoride, arsenic, selenium, and magnesium (see Figure 2). Thus, even if all free and complexed cyanide could be destroyed or recovered, the water quality of both mineral processing plants is not suitable for surface water discharge. This is due to the elevated concentrations of analytes such as arsenic [37], requiring further attenuation of contaminants using technologies such as nanofiltration [38], engineered wetlands [39], or other methods.

Advanced water treatment of cyanide-based mineral processing may be necessary under certain site conditions, such as dense clusters of processing activity that directly impact rivers [36]. This investigation primarily focused on establishing baseline treatment guidelines such as testing the effectiveness of different UV sources, optimizing peroxide dose requirements, and calculating rate constants to evaluate the overall effectiveness of cyanide destruction at mineral processing facilities in the Arequipa region. Currently, both mineral processing facilities evaluated in this research re-use contaminated water with minimal treatment. For example, both sites store waste cyanidation effluents onsite, exposing them to natural sunlight for extended periods of time (days to weeks) and yet these waters still contain elevated concentrations of cyanide (Figure 2). If cyanide can be effectively neutralized, other treatment processes may be performed to further elevate water quality. Because the Arequipa region has significant solar radiation [25], the first goal was to test the destruction of cyanide using ambient UV irradiation in combination with peroxide. However, little support for this type of treatment option was found (Figure 3a) as a rapid destruction method for treating cyanide-containing effluents. This is in contrast to other work that reportedly used simulated natural UV intensities and found rapid degradation of free cyanide and thiocyanates [40]. This result may be due to the UV wavelengths used in our study (285 nm), which fall in the UVB spectrum, whereas Mediavilla et al. [40] used a UVC lamp, which emits at shorter wavelengths (254 nm). However, Mediavilla et al. [40] also reported an irradiance of 26 mW/cm^2 , which is two orders of magnitude higher to that natural UV irradiation (0.2 mW/cm^2). Nonetheless, no change was observed in this study in initial cyanide concentrations when residential-use UV lamp was used with an irradiance of 4.6 mW/cm^2 (Figure 3b). This result clearly demonstrates that when UV alone is used, much stronger UV intensities than what a residential UV lamp can deliver are needed to rapidly degrade cyanide via photocatalytic oxidation. If rapid destruction is not a priority, then passive photocatalytic oxidation with peroxide may be a low-cost solution in processing plants that have downtime between each batch of ore. However, a variety of factors should be considered when attempting treatment in this manner, including sunlight intensity, turbidity, temperature, and depth of the water column. An additional factor for consideration is the presence of cyanide-containing compounds, such as thiocyanates and metal-cyanide complexes, which have slower degradation rates than free cyanide [17,40]. Furthermore, while cyanide-containing compounds, like thiocyanates, may be less toxic, their destruction and neutralization must be considered for any practical treatment option.

The time series analysis of the effects of peroxide alone and in combination with a UV lamp (Figure 3c) clearly demonstrates the need for above ambient UV intensities to accelerate degradation of free cyanide. This result is not surprising, considering that UV breaks the central bond of peroxide to yield $\cdot\text{OH}$ radicals [20]. However, when high strength cyanide-containing effluents are encountered, the reaction time takes significantly

longer (Figure 4). Thus, it is evident that under circumstances that require rapid turnover of process waters for cyanidation, a catalyst may be needed. When a TiO_2 photocatalyst was used in combination with low stoichiometric additions of cyanide to peroxide in a CPC, significantly higher degradation of high strength cyanide effluents ($>1\text{g/L CN}^-$) was observed within a 20 min period ($82.1\% \pm 5.2\%$ and $89.9\% \pm 1.9\%$ at 50 mg/L and 500 mg/L TiO_2) (Figure 5), with destruction efficiencies significantly correlated with peroxide dose (Figure 6). This result suggests that the UV- H_2O_2 - TiO_2 combination is effective for rapidly degrading high strength cyanide effluents, using minimal chemical addition, and should be explored further at the pilot scale.

Titanium dioxide combined with UV has been postulated to not have a high enough quantum yield to generate sufficient $\cdot\text{OH}$ radicals to enable efficient degradation [31]. This is exemplified by Mohammadi-Moghamadam et al. [26], which showed that the best removal efficiency obtained (using 300 mg/L CN^- starting concentration and 250 mg/L of substrate-stabilized TiO_2 particles) was $\sim 38\%$ destruction after 1 h and $\sim 75\%$ after 4 h. Other studies have also shown low degradation efficiencies: Kim et al. [27] reached $\sim 62\%$ removal of 27 mg/L CN^- starting concentration using high intensity UV and 50 mg/L Degussa P25-type TiO_2 after 5 h. However, because rate constants were not reported in these studies, it is difficult to make direct comparisons with the results obtained in this investigation. Nonetheless, the reason why such rapid degradation with the combinations of UV, peroxide, and TiO_2 was observed in this study might be explained by the interaction of excited TiO_2 particles on water molecules that form the solvent cage around $\cdot\text{OH}$ radicals [21]. The excited TiO_2 particles might break the solvent cage around the $\cdot\text{OH}$ radicals, thereby liberating the $\cdot\text{OH}$ radical to react with cyanide molecules. However, this investigation specifically focused on the destruction of free cyanide. Future work should characterize these effects on total cyanide, which may contain significant weak acid dissociable (WAD) and strong acid dissociable (SAD) metal cyanide species. Lastly, a full characterization of transformation byproducts is needed for our two main treatment combinations (i.e., UV/ H_2O_2 and UV/ H_2O_2 / TiO_2) in order to ascertain what downstream unit processes are needed to remove metals and nitrogen species (e.g., cyanate and ammonia).

5. Conclusions

Cyanidation process water is minimally treated at mineral processing facilities in the Arequipa region, where processed water is rich in inorganic contaminants and heavy metals, making it unfit for discharge to the environment. This water is typically reused by plant operators without any consideration on how polluted versus clean water might affect process efficiency. Thus, several UV and hydrogen peroxide-based treatment methods were tested, concluding that just by adding small amounts of hydrogen peroxide to cyanide effluent in the presence of solar UV irradiation is better than not using peroxide with a higher intensity UV lamp. However, this result was not practical for the timescales that are needed by operational scheduling. A combination of 1:1 stoichiometric addition of peroxide and higher intensity UV was found to be advantageous where high cyanide concentration effluents are encountered but were found to take ~ 5 h to reach complete destruction. The use of a titanium dioxide photocatalyst was found to be highly effective at increasing destruction rate, with minimal addition of peroxide, within a 20 min period. Further research should evaluate the effectiveness of current effluent water quality at processing plants versus treated water on gold extraction efficiency in ore, as well as the destruction of additional breakdown products during advanced oxidation.

Supplementary Materials: The following are available online at <https://www.mdpi.com/article/10.3390/su13179873/s1>, Figure S1: The effect of CuO on cyanide destruction in real mining wastewater.

Author Contributions: Conceptualization, D.C.V., J.V., L.A.F., V.H., F.N.A.-H., H.G.P.-C. and C.B.; data curation, D.C.V., J.V. and V.H.; formal analysis, D.C.V., J.V., L.A.F. and F.D.A.-Z.; funding acquisition, J.V., L.A.F., H.G.P.-C. and C.B.; investigation, D.C.V., J.V., L.A.F., V.H., F.N.A.-H., A.M., N.M.S., H.G.B.-S., F.D.A.-Z. and C.B.; methodology, D.C.V., J.V., V.H., F.N.A.-H. and C.B.; project administration, H.G.P.-C. and C.B.; resources, H.G.B.-S., F.D.A.-Z., H.G.P.-C. and C.B.; supervision, D.C.V., J.V. and H.G.P.-C.; validation, D.C.V.; visualization, D.C.V.; writing—original draft, D.C.V.; writing—review and editing, D.C.V., J.V., L.A.F., V.H., F.N.A.-H., A.M., N.M.S., P.A.G.-C., F.D.A.-Z., H.G.P.-C. and C.B. All authors have read and agreed to the published version of the manuscript.

Funding: This research was funded by the Center for Mining Sustainability, Arequipa, Peru.

Institutional Review Board Statement: Not applicable.

Informed Consent Statement: Not applicable.

Data Availability Statement: Data is available upon request.

Acknowledgments: The authors thank the valuable contributions from Autoridad Nacional del Agua (Peru) and the Center for Sustainable Mining. This work is dedicated to Felix Cuadros (R.I.P.) for his mentorship of both students and faculty in the broader research theme of metal-impaired environments. We additionally thank N. Rothe, T. Cath, H.E.G. Zenteno, and H.V.B. Tamayo.

Conflicts of Interest: The authors declare no conflict of interest.

References

1. MINEM Ministerio de Energía y Minas (MINEM). *Anuario Minero 2019*; MINEM: Lima, Peru, 2020; Volume 1, pp. 62–65.
2. Diringer, S.E.; Feingold, B.J.; Ortiz, E.J.; Gallis, J.A.; Araújo-Flores, J.M.; Berky, A.; Pan, W.K.Y.; Hsu-Kim, H. River transport of mercury from artisanal and small-scale gold mining and risks for dietary mercury exposure in Madre de Dios, Peru. *Environ. Sci. Process. Impacts* **2015**, *17*, 478–487. [CrossRef] [PubMed]
3. Fraser, B. Peruvian gold rush threatens health and the environment. *Environ. Sci. Technol.* **2009**, *43*, 7162–7164. [CrossRef]
4. Fritz, M.M.C.; Maxson, P.A.; Baumgartner, R.J. The mercury supply chain, stakeholders and their responsibilities in the quest for mercury-free gold. *Resour. Policy* **2016**, *50*, 177–192. [CrossRef]
5. Kahhat, R.; Parodi, E.; Larrea-Gallegos, G.; Mesta, C.; Vázquez-Rowe, I. Environmental impacts of the life cycle of alluvial gold mining in the Peruvian Amazon rainforest. *Sci. Total Environ.* **2019**, *662*, 940–951. [CrossRef] [PubMed]
6. Bebbington, A.J.; Bury, J.T. Institutional challenges for mining and sustainability in Peru. *Proc. Natl. Acad. Sci. USA* **2009**, *106*, 17296–17301. [CrossRef]
7. Fraser, J. Mining companies and communities: Collaborative approaches to reduce social risk and advance sustainable development. *Resour. Policy* **2018**. [CrossRef]
8. Salem, J.; Amonkar, Y.; Maennling, N.; Lall, U.; Bonnafoos, L.; Thakkar, K. An analysis of Peru: Is water driving mining conflicts? *Resour. Policy* **2018**. [CrossRef]
9. Dunlap, A. “Agro sí”, mina NO! the Tia Maria copper mine, state terrorism and social war by every means in the Tambo Valley, Peru. *Polit. Geogr.* **2019**, *71*, 10–25. [CrossRef]
10. Merkel, A. Arequipa, Peru Climate. Available online: <https://en.climate-data.org/south-america/peru/arequipa/arequipa-3078/#:~:text=Theclimatehereisclassified,inchofprecipitationfallsannually> (accessed on 1 August 2021).
11. Government of Peru. Supreme Decret NO. 106-2021-PCM. *El Peru*. **2021**, *28 May*, 7–8. Available online: <https://busquedas.elperuano.pe/normaslegales/decreto-supremo-que-declara-el-estado-de-emergencia-en-los-d-decreto-supremo-n-106-2021-pcm-1957547-2/> (accessed on 25 August 2021).
12. Ramos, U.J.; Flores, T.H. Contaminación de los ríos Coralaque y Tambo en el Departamento de Moquegua. *OPERACIONES Emerg. Nac.* **2020**, 1–21. Available online: <https://www.indec.gov.pe/wp-content/uploads/2020/02/INFORME-DE-EMERGENCIA-N%C2%BA-245-31MAR2020-CONTAMINACI%C3%93N-DE-LOS-RIOS-CORALAEQUE-Y-TAMBO-EN-EL-DEPARTAMENTO-DE-MOQUEGUA-10.pdf> (accessed on 25 August 2021).
13. MINSA. Reglamento de la Calidad del Agua para Consumo Humano. *Minist. Salud. Dir. Gen. Salud Ambient.* **2011**, 031-2010-S, 1–45. Available online: http://www.digesa.minsa.gob.pe/publicaciones/descargas/Reglamento_Calidad_Agua.pdf (accessed on 25 August 2021).
14. MINAM. Aprueban Estándares de Calidad Ambiental (ECA) para Agua y establecen Disposiciones Complementarias. *El Peru*. **2017**, *7 June*, 10–19. Available online: <https://busquedas.elperuano.pe/normaslegales/aprueban-estandares-de-calidad-ambiental-eca-para-agua-y-e-decreto-supremo-n-004-2017-minam-1529835-2/> (accessed on 25 August 2021).
15. Bebbington, A.; Williams, M. Water and Mining Conflicts in Peru. *Mt. Res. Dev.* **2008**, *28*, 190–195. [CrossRef]
16. Fraser, J. Peru Water Project : Cerro Verde Case Study Mining-Community Partnership To Advance Progress on Sustainable Development Goal 6. *Can. Int. Resour. Dev. Inst.* **2017**, 1–9. Available online: <https://cirdi.ca/wp-content/uploads/2017/09/Cerro-Verde-Case-Study-.pdf> (accessed on 25 August 2021).

17. Dzombak, D.A.; Ghosh, R.S.; Wong-Chong, G.M. *Cyanide in Water and Soil: Chemistry, Risk, and Management*; CRC Press: Boca Raton, FL, USA, 2006; ISBN 9781566706667.
18. Young, C.A.; Jordan, T.S.; Tech, M. Cyanide Remediation: Current and Past Technologies. In Proceedings of the 10th Annual Conference on Hazardous Waste Research, Manhattan, Kansas, 23–24 May 1995; 2006; pp. 104–129.
19. Vogels, G.D.; Uffink, L.; van der Drift, C. Cyanate decomposition catalyzed by certain bivalent anions. *Recueil* **1970**, *80*, 500–508. [[CrossRef](#)]
20. Linden, K.G.; Rosenfeldt, E.J. Ultraviolet light processes. In *Water Quality & Treatment: A Handbook on Drinking Water*; Edzwald, J.K., Ed.; American Water Works Association: Denver, CO, USA, 2011; pp. 18.1–18.45.
21. Oppenländer, T. *Photochemical Purification of Water and Air—Advanced Oxidation Processes (AOPs): Principles, Reactions Mechanisms, Reactor Concepts*; Wiley-VCH Verlag: Amsterdam, The Netherlands, 2003.
22. Kim, Y.J.; Qureshi, T.I.; Min, K.S. Application of advanced oxidation processes for the treatment of cyanide containing effluent. *Environ. Technol.* **2003**, *24*, 1269–1276. [[CrossRef](#)]
23. Monteagudo, J.M.; Rodríguez, L.; Villaseñor, J. Advanced oxidation processes for destruction of cyanide from thermoelectric power station waste waters. *J. Chem. Technol. Biotechnol.* **2004**, *79*, 117–125. [[CrossRef](#)]
24. Fungene, T.; Groot, D.R.; Mahlangu, T.; Sole, K.C. Decomposition of hydrogen peroxide in alkaline cyanide solutions. *J. South. African Inst. Min. Metall.* **2018**, *118*, 1259–1264. [[CrossRef](#)]
25. Young, A.H.; Knapp, K.R.; Inamdar, A.; Hankins, W.; Rossow, W.B. The International Satellite Cloud Climatology Project H-Series climate data record product. *Earth Syst. Sci. Data* **2018**, *10*, 583–593. [[CrossRef](#)]
26. Mohammadi-Moghadam, F.; Sadeghi, M.; Masoudipour, N. Degradation of Cyanide using Stabilized S, N-TiO₂ Nanoparticles by Visible and Sun Light. *J. Adv. Oxid. Technol.* **2018**, *21*. [[CrossRef](#)]
27. Kim, S.H.; Lee, S.W.; Lee, G.M.; Lee, B.T.; Yun, S.T.; Kim, S.O. Monitoring of TiO₂-catalytic UV-LED photo-oxidation of cyanide contained in mine wastewater and leachate. *Chemosphere* **2016**, *143*, 106–114. [[CrossRef](#)]
28. Stein, L.Y. Cyanate fuels the nitrogen cycle. *Nature* **2015**, *524*, 43–44. [[CrossRef](#)]
29. Childs, L.P.; Ollis, D.F. Is photocatalysis catalytic? *J. Catal.* **1980**, *66*, 383–390. [[CrossRef](#)]
30. Pruden, A.L.; Ollis, D.F. Photoassisted heterogeneous catalysis: The degradation of trichloroethylene in water. *J. Catal.* **1983**, *82*, 404–417. [[CrossRef](#)]
31. Sun, L.; Bolton, J.R. Determination of the quantum yield for the photochemical generation of hydroxyl radicals in TiO₂ suspensions. *J. Phys. Chem.* **1996**, *100*, 4127–4134. [[CrossRef](#)]
32. Read, R.W.; Vuono, D.C.; Neveux, I.; Staub, C.; Grzymski, J.J. Coordinated downregulation of the photosynthetic apparatus as a protective mechanism against UV exposure in the diatom *Corethron hystrix*. *Appl. Microbiol. Biotechnol.* **2019**, *103*, 1837–1850. [[CrossRef](#)]
33. Lubin, D.; Jensen, E.H.; Gies, H.P. Global surface ultraviolet radiation climatology from TOMS and ERBE data. *J. Geophys. Res. Atmos.* **1998**, *103*, 26061–26091. [[CrossRef](#)]
34. Tarras-Wahlberg, N.H.; Flachier, A.; Lane, S.N.; Sangfors, O. Environmental impacts and metal exposure of aquatic ecosystems in rivers contaminated by small scale gold mining: The Puyango River basin, southern Ecuador. *Sci. Total Environ.* **2001**, *278*, 239–261. [[CrossRef](#)]
35. Ashe, K. Elevated mercury concentrations in humans of madre de dios, Peru. *PLoS ONE* **2012**, *7*, e33305. [[CrossRef](#)]
36. Marshall, B.G.; Veiga, M.M.; da Silva, H.A.M.; Guimarães, J.R.D. Cyanide Contamination of the Puyango-Tumbes River Caused by Artisanal Gold Mining in Portovelo-Zaruma, Ecuador. *Curr. Environ. Heal. Rep.* **2020**. [[CrossRef](#)]
37. Eisler, R.; Wiemeyer, S.N. Cyanide Hazards to Plants and Animals from Gold Mining and Related Water Issues. In *Reviews of Environmental Contamination and Toxicology*; Ware, G.W., Ed.; Springer-Verlag: New York, NY, USA, 2004; Volume 183, pp. 21–54. ISBN 9781461264941.
38. Andrade, L.H.; Aguiar, A.O.; Pires, W.L.; Miranda, G.A.; Teixeira, L.P.T.; Almeida, G.C.C.; Amaral, M.C.S. Nanofiltration and reverse osmosis applied to gold mining effluent treatment and reuse. *Brazilian J. Chem. Eng.* **2017**, *34*, 93–107. [[CrossRef](#)]
39. Gessner, T.P.; Kadlec, R.H.; Reaves, R.P. Wetland remediation of cyanide and hydrocarbons. *Ecol. Eng.* **2005**, *25*, 457–469. [[CrossRef](#)]
40. Mediavilla, J.J.V.; Perez, B.F.; De Cordoba, M.C.F.; Espina, J.A.; Ania, C.O. Photochemical degradation of cyanides and thiocyanates from an industrial wastewater. *Molecules* **2019**, *24*, 1373. [[CrossRef](#)] [[PubMed](#)]